Oxidative electrofluorochromism of rhodamine in electropolymerized rhodamine-carbazole dyads

Jennifer Calderon-Mora, Baptiste Maillot, Jean-Frédéric Audibert, Philippe Decorse, Isabelle Bonnamour, Roxanne Mollandin de Boissy, Florian Guier, Ulrich Darbost, Vitor Brasiliense, Fabien Miomandre

Oxidative electrofluorochromism of rhodamine in electropolymerized rhodamine-carbazole dyads

Jennifer Calderon-Mora [a], Baptiste Maillot [a], Jean-Frédéric Audibert [a], Philippe Decorse [b], Isabelle Bonnamour [c], Roxanne Mollandin de Boissy [d], Florian Guier [d], Ulrich Darbost [d], Vitor Brasiliense [a,*], Fabien Miomandre [a,*]

[a] Université Paris-Saclay, ENS Paris-Saclay, CNRS, PPSM, 4 avenue des sciences, GIF-SUR-YVETTE 91190, France
[b] Université Paris-Cité, ITODYS, 15 rue Jean de Baïf, PARIS 75013, France
[c] Institut Lumière Matière, Université Lyon 1, 10 rue Ada Byron, VILLEURBANNE 69622, France
[d] Institut de Chimie et Biochimie Moléculaires et Supramoléculaires, Université Lyon 1, 1 rue Victor Grignard, VILLEURBANNE 69600, France

ARTICLE INFO

Keywords:
Rhodamine
Carbazole
Conducting polymer
Electrofluorochromism
Electrochromism

ABSTRACT

A rhodamine-carbazole dyad has been synthesized and electropolymerized to generate thin films. The spectroelectrochemical properties of the resulting polymer are investigated both in absorption and emission. We show that the luminescence of the rhodamine unit is partially quenched by the carbazole moiety and this quenching is strongly enhanced upon oxidation. A reversible switch of the emission intensity between two redox states is demonstrated, but the stability is strongly dependent on the film thickness and proportion of carbazole in the polymerization medium. This luminescence quenching can be used to follow the electropolymerization reaction since a strong decrease of intensity occurs as soon as the oxidative coupling reaction starts.

1. Introduction

Electrofluorochromism, defined as the electrochemical modulation of fluorescence [1], conveniently enables redox events to be reported optically. Due to emerging applications in displays [2], sensors [3] and anti-counterfeiting [4], the interest in the field has sharply risen over the past few years. Emission modulation is often accompanied by electrochromic properties either in molecular or macromolecular systems [5,6]. Two main strategies are often used to design electrofluorochromic probes: they can be designed by either selecting redox active fluorophores or by associating redox units and fluorophores with electronically conducting linkers [7,8]. The use of conjugated polymers in this framework dates of approximately two decades with pioneering works of the groups of Kim [9,10] and Montilla [11,12] among others. The molecular engineering strategy can be divided into two categories: either the fluorescent or fluorogenic units are introduced as pendant groups on the conjugated backbone [13] or they are directly incorporated in the repetition unit [14]. Classical conjugated electropolymerizable units like thiophene [15], aniline [6], carbazole [16] and especially more recently triphenylamines [17–19] have been associated to various highly emissive units like fluorescein [20] or rhodamine (Rd) [21] to design electrofluorochromic polymers [22]. Dyes based on the association of rhodamine B (RhB) as a highly emissive unit and carbazole (Cz) as an electron-rich compound showed interesting electrochemical and color switching properties [23]. Indeed, electropolymerizable units consisting in rhodamine and carbazole dyads have been recently reported to display valuable electrochromic properties [24,25]. While no electrochemically monitored light emission investigation was reported so far, we suspected that interesting electrofluorochromic properties could emerge, revealing detailed electronic interaction between the elements of the dyad. In particular, we were interested in understanding if the light emission from Rd could be reversibly tuned in polymers, revealing an interesting pathway towards smart materials with application in displays.

Therefore, having in mind also possible applications to design macromolecular switchable junctions, we decided to investigate them more deeply using an original instrumental setup combining fluorescence microscopy with electrochemistry recently developed in our group [26]. This paper describes the electrofluorochromic properties of a conjugated polymer based on a Rd-Cz dyad (Scheme 1) that can be electropolymerized to make thin films. While electrofluorochromic properties upon reduction of Rd have been already reported [27], this is

* Corresponding authors.
E-mail addresses: vitor.brasiliense@ens-paris-saclay.fr (V. Brasiliense), mioman@ens-paris-saclay.fr (F. Miomandre).

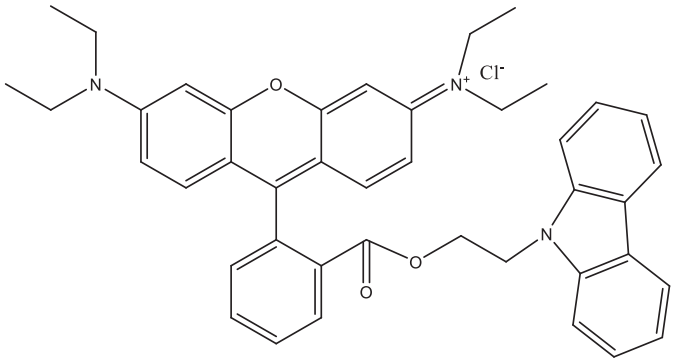

Scheme 1. Molecular structure of the RdCz dyad.

the first time to our knowledge that oxidative electrofluorochromism of this dye is demonstrated. We also show that the amount of carbazole in the final composition of the polymer is crucial to observe the phenomenon with a reasonable stability. The structural properties of the final materials are finely characterized by a combination of FTIR and XPS.

2. Experimental

2.1. Chemicals and materials

All chemicals were of analytical grade without further purification: Rhodamine B 95 %, Carbazole > 95 %, Boron trifluoride-diethyl etherate (BTFE), dichloromethane (DCM) and 1,2-dichloroethane (DCE) from Carlo Erba Reagents, tetrabutylammonium hexafluorophosphate 98 % ($TBAPF_6$) from TCI Chemicals, sodium carbonate (Na_2CO_3) from Prolab, ultrapure milli-Q water. For electrodeposition, the substrates used were 10 mm × 30 mm or 25 mm × 25 mm ITO-coated glass plates (from Solems) previously rinsed with ethanol.

Solvents were dried by conventional methods. Column chromatography was performed using a Combiflash. The reactions were monitored by TLC on a silica gel plate and visualized by UV light. The ^{1}H and ^{13}C NMR spectra were recorded on a Bruker DRX at 500 MHz in $CDCl_3$. Mass spectra were acquired on a LCQ Advantage ion trap instrument, detecting positive ions in ESI mode.

2.2. Electropolymerization of Rd-Cz

The poly(RdCz) films on ITO were synthesized *via* cyclic voltammetry (CV) or chronoamperometry (CA) techniques. A three-electrode cell assembly was utilized with a pseudo-reference electrode (Ag wire), counter electrode (Pt wire), and working electrode (ITO). The electrochemical cell was filled with a solution containing 0.1 M (unless stated otherwise) RdCz dyad + x_w% ($1 < x < 10$) of pure carbazole (Cz), dissolved in DCM+BTFE as solvent (1 drop of BTFE per ~ 2 mL of solution), and 0.1 M $TBAPF_6$ as the supporting electrolyte. The RdCz solution exhibited a bright pink color. Electropolymerization was usually achieved via CV by cycling the potential between 0.3 V and 1.5 V for five cycles at a scan rate of 0.1 V s^{-1}. It was also achieved via CA by applying 1.5 V for 60 s.

After polymerization, the polymer films on ITO were rinsed with DCM and ethanol. The electrochemical characterization of poly(RdCz) was performed by CV in 0.1 M $TBAPF_6$ DCM solution (monomer free electrolyte). The measurements were performed with a CH Instruments potentiostat (CHI 600).

2.3. Combined electrochemical and optical microscopy set-up

All spectroelectrochemical experiments were conducted in a set-up coupling an electrochemical cell with an inverted fluorescence microscope as shown in Fig. 1.

Electrochemistry – Electrochemical measurements were performed using a homemade spectroelectrochemical cell mounted on top of an inverted optical microscope. A platinum wire and an Ag wire were used as the counter and pseudo-reference electrodes, respectively. The set-up was used in a three-electrode configuration employing a transparent conductive substrate (ITO coated glass coverslips) as the working

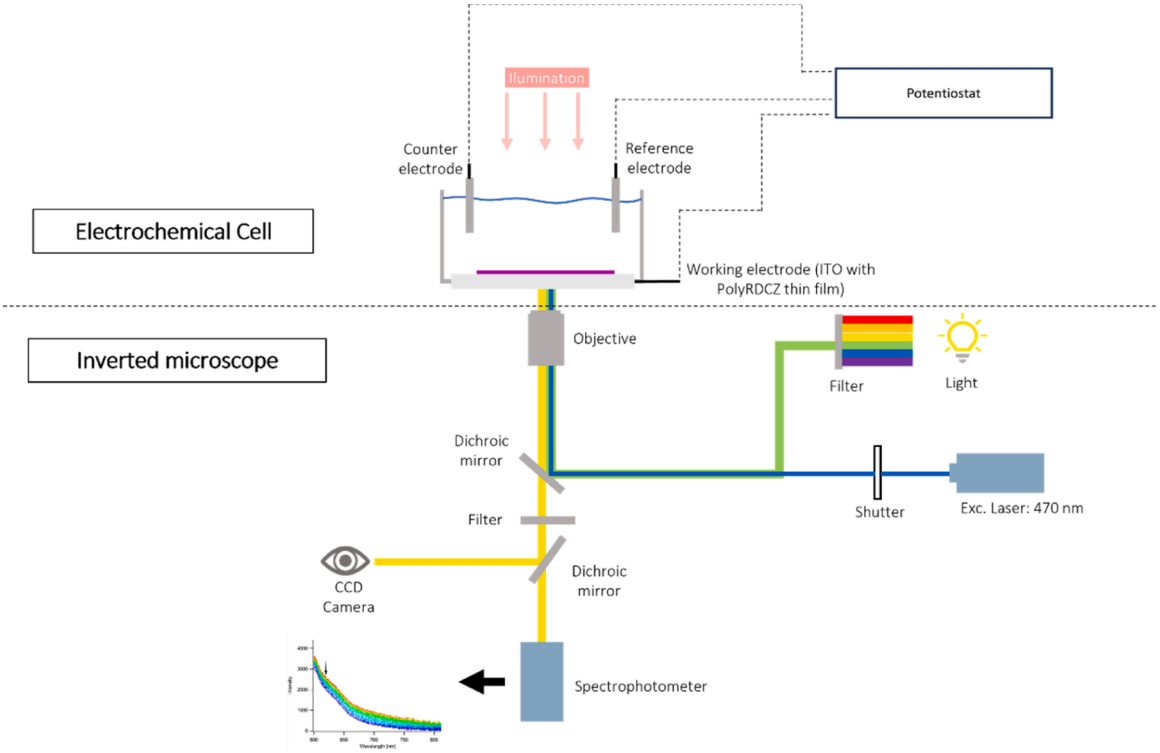

Fig. 1. Experimental set-up for combined electrochemical and optical (absorption and fluorescence) experiments.

electrode. Measurements were carried out with a VersaSTAT4 potentiostat (HTDS) driven by VersaStudio software (HTDS).

Optical measurements – Optical measurements were performed on an inverted microscope (Ti Eclipse Nikon) with a 40× NA 0.60 objective in a wide-field epi-illumination configuration. Excitation sources used were a Hg lamp (Intensilight Nikon) with a band pass excitation filter (BP 561-14 nm) and m-Cherry dichroic mirror or a pulsed laser diode at 474 nm (LDH-P-C-470B, 40 MHz, Picoquant) with a pulse width of 150 ps. In order to minimize photobleaching effects, the excitation sources used for each experiment were selected by opening and closing the respective shutters controlled manually or triggered with the help of an Arduino board. Emitted light is collected through a long pass emission filter (LP 595 nm). Acquisition time-lapses are carried out using a CCD Pixel Fly camera from PCO under the μManager open-source software. Emission spectra are recorded with an Ocean Optics spectrometer coupled to the microscope with an UV-Vis (400 μm diameter) optical fiber plus collimator placed in an intermediate image plane, with a 60 μm mode field diameter in the sample plane centered around the tip.

Lifetime measurements were acquired using Time-Correlated Single Photon Counting (TCSPC) technique where photons are recorded in TTTR (Time-Tagged Time Resolved) [28] mode at 2.5 MHz (or 10 Mz) using a TCSPC 260Nano PCIe card from Picoquant with a global IRF resolution of 550 ps. Emitted light is collected through a long pass emission filter (LP 520 nm) with a graded index multimode fiber APD (MPD-CCTC, Picoquant) with a mode field diameter of 60 μm in sample plane.

2.4. X-ray photoelectron spectroscopy (XPS)

XPS measurements were performed using a K-Alpha$^+$ spectrometer (ThermoFisher Scientific, East Grinstead, UK) operated in the constant analyzer energy mode, and equipped with a micro-focused and monochromatic Al Kα X-ray source (1486.6 eV, spot size: 400 μm, 12 kV, 6 mA) and a flood gun (for insulating samples). The samples were clipped onto the sample holder and outgassed overnight in the fast-entry lock. The step size and pass energy were set to 1 eV/200 eV and 0.1 eV/40 eV for the survey and the high resolution regions, respectively. Data acquisition and processing was done using Avantage software (ThermoFisher Scientific), version 5.9902. The surface chemical composition was determined by using the manufacturer sensitivity factors.

2.5. Fourier-transform infrared spectroscopy (FTIR)

ATR-FTIR analysis was carried out on a Nicolet iS50 FT-IR (Thermo Scientific) spectrometer. Air was used for the background spectrum. The electropolymerized sample was a thin film (~ 150 nm thickness) on a thin ITO slide. Spectra were recorded with a total of 32 scans.

2.6. Atomic force microscopy (AFM)

AFM images were collected on a Icon Dimension Atomic Force Microscope (Bruker) equipped with Si PointProbePlus tips (PPP-NCHR, NanoSensors) operated on tapping mode.

2.7. Sample preparation

XPS samples were prepared by cyclic voltammetry as described in Section 2.3 with 5 cycles in the presence of 5 or 10 w% free carbazole. Static absorption and emission properties of poly(Rd-Cbz) layers were measured on samples obtained in the presence of 3 w% free carbazole. The same samples were characterized ex-situ using FTIR.

3. Results and discussion

3.1. Monomer synthesis

The synthesis of the Rd-Cz monomer is based on a previously reported protocol [25], but the purification and the yield were improved. The purification was realized on a combiflash device using a DCM/Methanol 9/1 gradient. Rd-Cz was finally obtained in 75 % yield. All NMR and MS characterizations of the product can be found in Supplementary information (Figs. S1–S5).

3.2. Electropolymerization

All attempts to electropolymerize pure Rd-Cz dyad failed, despite the use of a high concentration of the monomer and addition of BTFE to get rid of residual nucleophilic species. Difficulties to electropolymerize N-substituted carbazoles were already reported in the literature [29], but they are further reinforced here due to the cationic form of Rd in the dyad which disfavors the formation of the cation radical on the carbazole moiety to initiate the polymerization.

Over the course of these experiments, however, we noticed that the addition of a small amount of Cz in the initial mixture triggered the electropolymerization. The presence of free carbazole enables statistical polymers to form, as indicated in Scheme 2. It can be noticed that RdCz had been already incorporated into conjugated polymer backbone by a copolymerization process in a previous report [30]. Therefore, we focused the investigation on the electropolymerization of a mixture containing small amounts of Cz, typically 5–10 $\%_w$, a reasonable limit to keep the spectroelectrochemical and emission properties. The first cycles of a typical cyclic voltammogram, obtained with 3 %w carbazole, are shown in Fig. 2A. The increase in the anodic current observed at sequential cycles indicates an increase of the electrode area and appearance of an electroactive entity on the electrode. These results are consistent with an electropolymerization reaction, confirmed by the appearance of a colored deposition on ITO. The thickness of the resulting layers is characterized ex-situ with the help of AFM (vide infra). Fig. 2B shows the evolution of the resulting layer thickness with the number of cycles in the CV, which is almost linear in the explored range.

3.2.1. Electrochemical characterization

The electrochemical properties of the resulting film are further characterized by transferring the modified electrode to a monomer-free electrolyte solution (0.1 M $TBAPF_6$ in DCM) and cycling it anodically. As indicated in Fig. 2C, an anodic wave can be readily detected in the

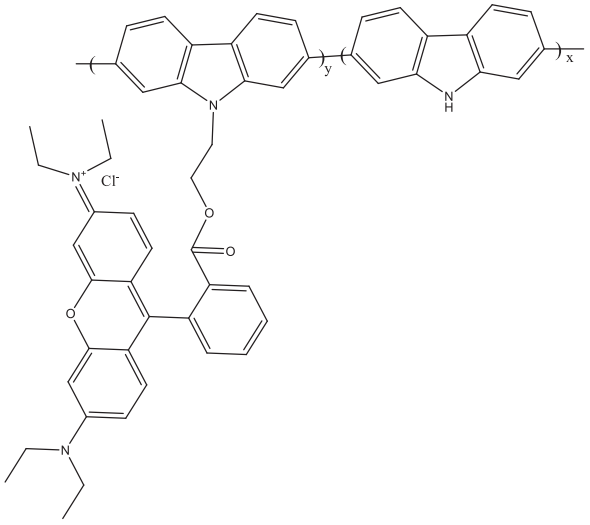

Scheme 2. Structure of poly(Rd-Cz).

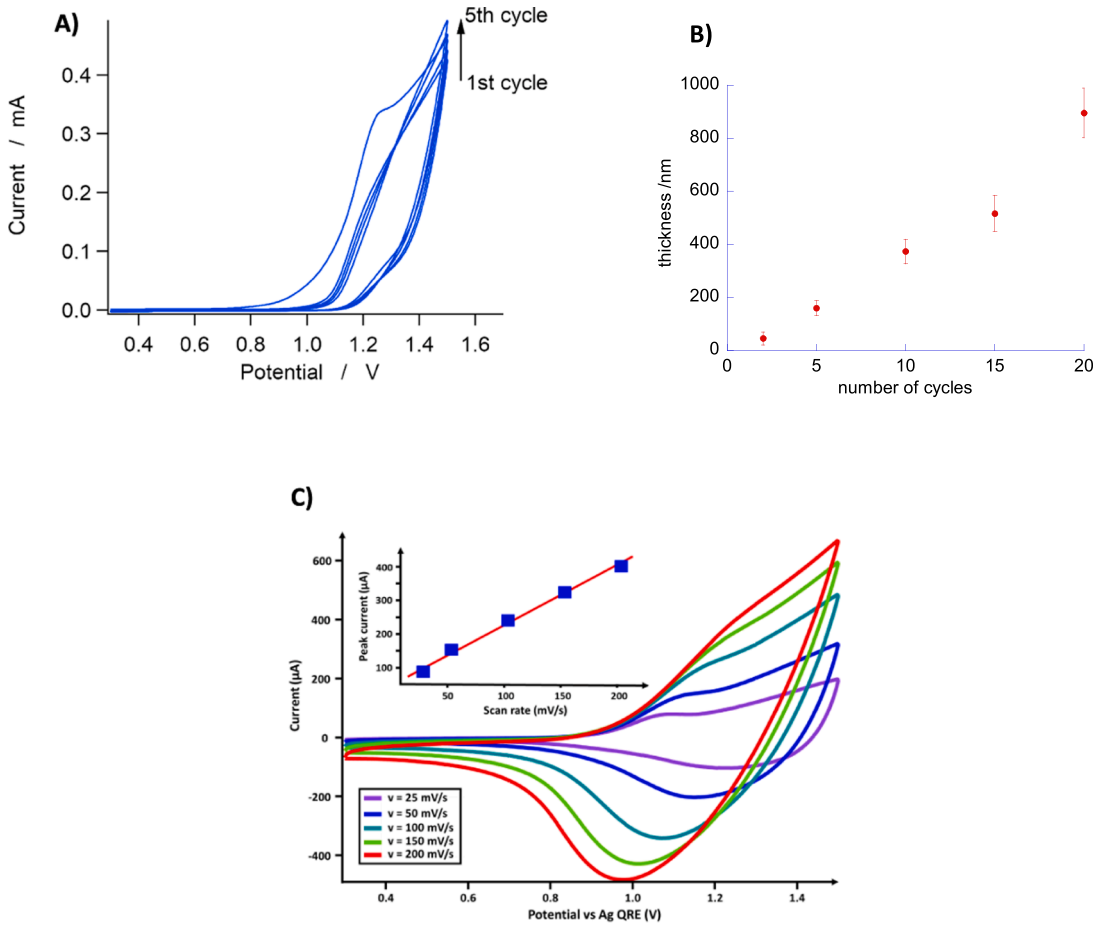

Fig. 2. A) Electropolymerization by cyclic voltammetry (0.1 V/s) of RdCz 0.1 M + 3 %Cz in DCM and 100 mM $TBAPF_6$. B) Film thickness measured by ex situ AFM vs. number of electropolymerization cycles. C) Electrochemical characterization of poly(RdCz) made with experimental conditions of A) on ITO in DCM + $TBAPF_6$ at various scan rates and plot of anodic peak current vs. scan rate (inset).

1.2–1.4 V (vs. Ag QRE) range. With respect to other substituted poly-Cz derivatives [31,32], this range is relatively high, suggesting that the oxidation process involves the cationic Rd unit in addition to the conjugated polymer backbone. Indeed, the presence of a positively charged moiety makes the polymer oxidation significantly more difficult.

The surface density of electroactive units (and therefore the polymer thickness) can be assessed using Eq. (1):

$$i_p = \frac{n^2F^2}{4RT}A\Gamma^* v = \alpha v \tag{1}$$

where i_p is the peak current, n the number of electrons exchanged, v is the scan rate, A is the electroactive area and Γ^* is the surface concentration of redox units. The linear fit (Fig. 2C, inset) indicates a redox process limited by the number of electroactive sites in the film. The determination of n and Γ^* can be performed using Faraday's law (2):

$$Q = nFA\Gamma^* \tag{2}$$

where Q is the charge deduced from integration of the voltammetric peak after subtracting the background current.

Combining Eqs. (1)–(2) leads to:

$$n = 4\frac{RT}{F}\frac{\alpha}{Q} \tag{3}$$

$$\Gamma^* = \frac{Q^2}{4RTA\alpha} \tag{4}$$

The slope of the linear fit in Fig. 2C ($\alpha = 1.8\ 10^{-3}$ F) and the measured redox charge ($Q = 0.55$ mC) lead to $n \approx 0.3$ and $\Gamma^* \approx 5 \times 10^{-9}$ mol.cm^{-2}. This latter value is consistent with a thin film of approximately 50 layers of redox sites and thus is in agreement with the measured thickness of 150 nm (Fig. S6) and the estimated size of the repeating unit (Fig. S7) [33]. The number of electrons exchanged is consistent with the usual doping level of conjugated materials as well. However, such analysis must be taken with care as it assumes fast kinetics, a homogeneous distribution of redox species in the film, and the non-dependency of Γ^* with the potential, which are conditions that may be not entirely fulfilled [34,35].

3.2.2. *Surface chemical characterization*

To gather more insight into the chemical nature of the electrodeposited layers XPS and FTIR experiments were done. As the electropolymerization reaction is operated from a mixture of free carbazole and dyads, we first used FTIR to confirm the presence of vibrations associated with rhodamine moieties, and later employed XPS to reveal details in its chemical composition.

FTIR. Poly(RdCz) was obtained from a solution containing 3 $\%_w$ free Cz and 5 electropolymerization cycles, leading to a layer of ca. 150 nm, as determined by AFM. In Fig. 3, we compare the FTIR spectra obtained from an electropolymerized layer with spectra made with the dyad powder and a pristine ITO sample. The presence of the RdCz moiety in the polymer is confirmed by the appearance of peaks at 1715 cm^{-1} associated to the carbonyl group of Rd, and at 1587 cm^{-1} and 1418 cm^{-1} associated to the aromatic rings [30]. These bands are clearly identified both in the monomer powder and the polymer film,

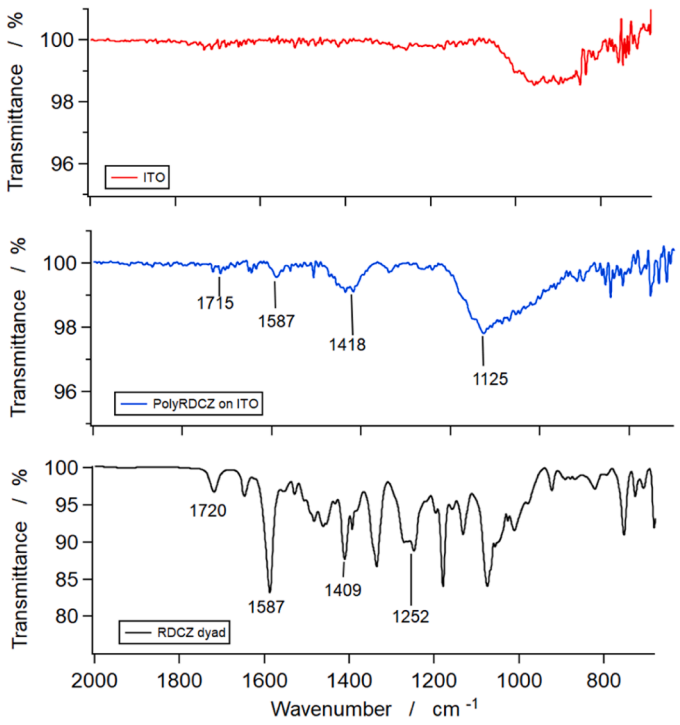

Fig. 3. FTIR spectra of bare ITO (top), poly(RdCz) on ITO (middle), and RdCz dyad powder (bottom), added as a reference.

despite small shifts in the wavenumbers ($< 10\ cm^{-1}$), commonly observed as a result of the modification of the local environment of the moieties when polymerized. These results confirm that, even in the presence of a relatively high (3 $\%_w$ i.e. 10 $\%_{mol}$ Cz) free carbazole, the electrodeposited polymer contains a reasonable proportion of rhodamine.

XPS. A more quantitative chemical analysis of the composition of the polymerized layers, revealing the influence of the free carbazole, can be performed by XPS.

XPS spectra were recorded on poly(RdCz) layers electropolymerized on ITO from solutions containing RdCz in the presence of various amounts of Cz. The full dataset can be found in Supporting information (Fig. S8), with typical results, obtained for electropolymerization in the presence of 10 $\%_w$ Cz, shown in Table 1.

The XPS data reveals interesting trends. First of all, significant amounts of chlorine are systematically observed in each sample, suggesting that Rd is present in its cationic form, which is consistent with NMR data (Supporting information, Fig. S1) of the dyad. Then, four types of carbon can be identified corresponding to aliphatic carbon, C═C, C-N and C═O by order of increasing energies. The C signal is very similar to what can be seen in Cz containing conjugated polymers [36]. Furthermore, the N signal can be decomposed into a main peak located at 399 eV and a weaker one at higher energy (404.8 eV) which is higher in energy than the usual value corresponding to C-N in Rd [30]. This energy shift could correspond to oxidized nitrogen due to carbazole doping with electrolyte. The presence of P and F in significant amounts and roughly at a 1:6 ratio testifies for the presence of the hexafluorophosphate counter-ion in the film, supporting the hypothesis of polymer doping.

Interesting trends can also be extracted by analyzing in the XPS spectra the influence of the free Cz to dyad ratio present in the electrodeposition medium ($\%_w$ $Cz_{(sol)}$). In particular, the proportion of unsubstituted carbazole to dyad monomers (x/y ratio, following the nomenclature introduced in Scheme 2) can be estimated based on XPS data. Indeed, as $\%_w Cz_{(sol)}$ is increased, so should the x/y ratio. On the basis of the structures (Scheme 2), the N/Cl ratio is expected to be related to x/y as:

$$\frac{N}{Cl} = 3 + \frac{x}{y} \quad (3)$$

Table 2 shows that the estimated proportions qualitatively agree with the expected trend.

Table 1
XPS data for poly(RdCz) on ITO electropolymerized with 10 $\%_w$ Cz in the reactional mixture (5 cycles from 0.3 to 1.5 V).

Element	Energy /eV	Atomic %
P 2p	135.9	1.3
Cl 2p	199.9	1.2
C 1s	284.0	41.2
C 1s A	285.0	24.9
C 1s B	286.3	6.3
C 1s C	288.5	3.0
C 1s D	290.8	1.2
N 1s	399.4	4.8
N 1s A	401.5	0.9
N 1s B	404.9	0.2
O 2p	532.0	7.7
F 1s	685.9	7.3

Table 2
x/y ratios determined by XPS from %N/%Cl ratio for various initial compositions of the reactional mixture for electropolymerization (5 cycles from 0.3 to 1.5 V).

Initial composition	%N/%Cl	x/y
RdCz 0.01 M + 5 w%CZ	3.1	0.1
RdCz 0.01 M + 8 w%CZ	3.4	0.4
RdCz 0.01 M + 10 w%Cz	5.1	2.1

3.3. Absorption and fluorescence

We next turned to the analysis of the absorption and emission properties of the poly(RdCz) layers. Both spectra are collected locally (typically on 10 μm × 10 μm zones), and repeated at several locations on the sample surface.

Absorption Properties. Typical absorption spectra are shown in Fig. S9, along with the absorption spectra of dyad solution and of polycarbazole. Although broader and slightly redshifted with respect to the dyad absorption bands, the main visible band of the dyad can be safely assigned to the Rd chromophore. Broad bands in the UV and NIR regions are also present albeit at lower intensity, which are attributed to the polycarbazole backbone. This assignment is made on the basis of the polycarbazole spectrum obtained under similar conditions.

A typical steady state emission spectrum of poly(RdCz) is shown in Fig. 4A, and shows a maximum at 610 nm, which is red-shifted compared to the emission of free RhB in DCM (585 nm). We assessed the homogeneity of the film by measuring at several (N = 7) different positions, obtaining ca. 80 % variation in the emission intensity. Although the emission may vary with the location under the microscope, a good correlation is observed between the emission intensity and the absorbance at the excitation wavelength (Fig. 4B), indicating that the photophysical properties are homogeneous throughout the film.

The emission lifetime is short (ca. 0.5 ± 0.05 ns) at the limit of the instrumental detection, and shows no signs of bleaching over 2 min (Fig. 4C). This value is much lower than the one of the dyad in solution (3.7 ns, similar as Rd alone), showing that the conjugated backbone is involved in a quenching process, through electron transfer mainly. Emission lifetime remains constant with time under continuous irradiation, precluding any variation of this quenching process in absence of electrochemical signal.

3.4. Electrochromism

Having characterized the properties of the polymer in absence of potential, we turned on the analysis of how to tune these properties according to the applied potential. The electrochromic properties of poly(RdCz) are first investigated by recording the UV–vis spectra of the layer at different anodic potentials, leading to the results shown in Fig. 5. The main absorption band located at 560 nm, assigned to the Rd chromophore, starts to decrease for electrode potentials higher than 1.2 V. Compared to the same experiment done with RhB in solution (Fig. S10), a very similar behavior can be observed, with an absorption gradually decreasing from the same potential. It shows that oxidation in poly(RdCz) involves the Rd unit, a behavior different from the one reported in analogous materials but where the Rd unit is not supposed to be cationic [24,25].

At higher potential values, a broad absorption band develops over the whole spectrum, which becomes approximatively uniform between 450 and 800 nm. This change, which can be assigned to the polycarbazole substructure oxidation is accompanied by the appearance of an orange coloration in the film. (see Fig. S11).

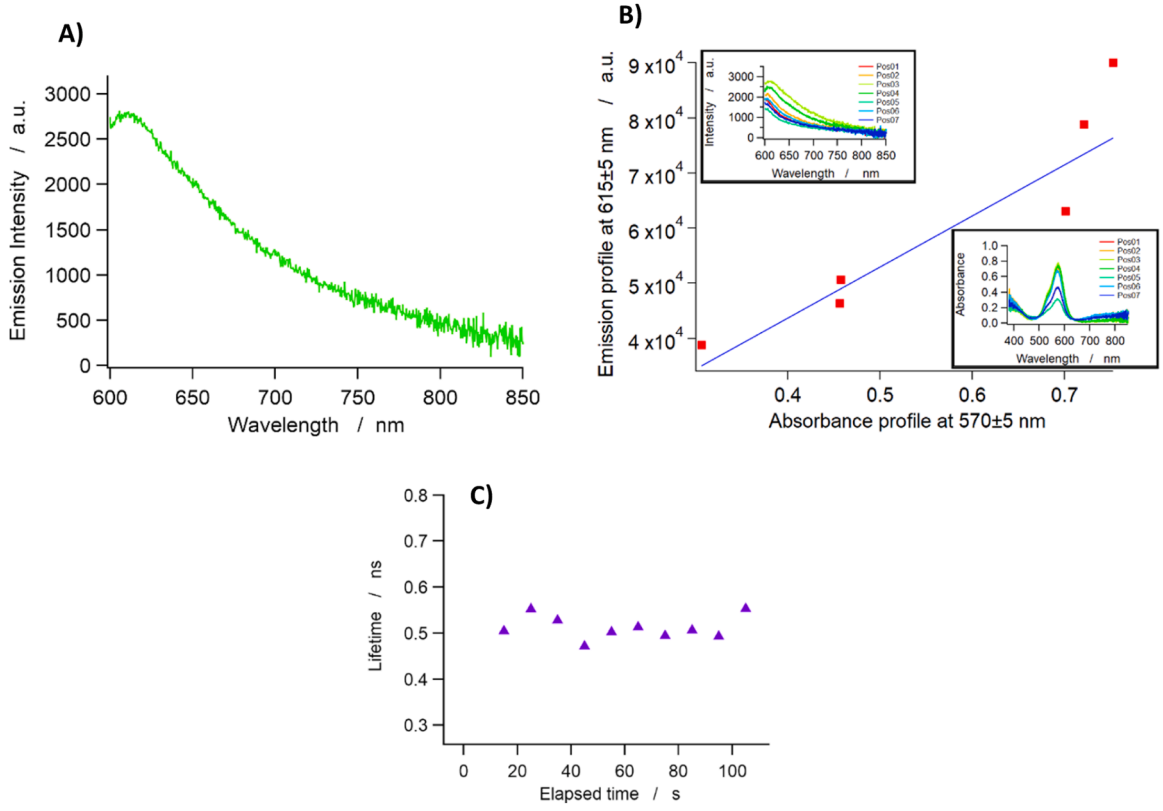

Fig. 4. A) Fluorescence spectrum of poly(RdCz). Excitation wavelength: 560 nm; B) Emission at 615 ± 5 nm vs. Absorbance at 570 ± 5 nm at different locations of a poly(RdCz) film electropolymerized on ITO. Inset top: Emission spectra at different positions (Excitation wavelength: 560 nm). Inset bottom: Absorbance spectra at different positions. C) Emission lifetime of a poly(RdCz) film prepared with a 0.1 M RDCZ + 3 % CZ solution vs. time under continuous irradiation at the excitation wavelength of 560 nm.

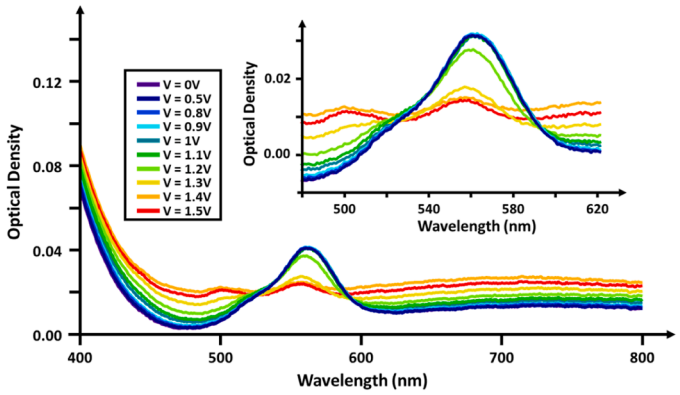

Fig. 5. Absorption spectra of poly(RdCz) prepared with a 0.1 M RdCz + 10 w% CZ solution in DCM at potentials spanning 0 (purple) to 1.5 V (red).

3.5. Electrofluorochromism

The UV-Vis spectra recorded in the previous sections highlights differences in the absorption properties of the polymer depending on its redox state, which has been occasionally used in literature to develop smart materials and sensors [25]. Owing to the fluorescence properties of the material, these changes are expected to be accompanied by potential-dependent emission properties, i.e an electrofluorochromic behavior. As indicated in the scheme of Fig. 1, the electropolymerized poly(RdCz) film on ITO is used as the working electrode in a home-made electrochemical cell positioned in the focal plane of an inverted epi-fluorescence microscope. This configuration allows us to follow the variation of the emission intensity of the poly(RdCz) film in real-time at different potentials with high spatial resolution.

Emission variation with applied potential. The film emission spectra are recorded at several potentials, using chronoamperometry steps of 10 s, which are made progressively more anodic (Fig. 6A). As anticipated on the basis of the electrochromic properties of the film, its emissive properties are strongly potential dependent, as long as a threshold is crossed. Indeed, as indicated in Fig. 6B, anodic polarization at 1.0 V is already enough to substantially decrease the fluorescence emission. Such changes are more clearly measured at 1.5 V, and at 2.0 V we observe poor fluorescence recovery, a behavior assigned to film degradation.

In most electrofluorochromic applications, reversible switches are sought, therefore a potential where emission is modified yet the film remains intact must be found. Such a tradeoff seems to exist near 1.5 V, which leads to a strong decrease of the fluorescence signal (30 %), followed by full recovery when the potential is brought back to 0 V.

Based on these potential values, a stability analysis is carried out for these limit potentials, aiming at determining optimal conditions to observe electrofluorochromism. The analysis is focused on two parameters: the amount of Cz in the polymerization medium and the film thickness. We have checked that these two parameters are not interdependent (see Table S1 in Supporting information).

Film Thickness. The influence of film thickness is shown in Fig. S12A. When the film is very thin (2 polymerization cycles corresponding to a thickness of 18± 9 nm), the coating is not homogeneous and no clear modulation can be observed (curve a). Increasing the number of polymerization cycles to 5 (47± 3 nm) enables a much better performance to be observed, with reversible monitoring of the fluorescence (curve b, identical to Fig. 6B). As the film becomes thicker, the modulation becomes more hectic and much less reversible (curves c–d). Fluorescence quenching is observed thus showing that oxidation takes place but without recovery when the potential is stepped back. This shows that the electrochemical reaction becomes irreversible when the film thickness increases, probably in line with a disordered structure.

Influence of Cz amount. Having identified optimal values for the thickness and applied potential, we focused on the influence of the Cz amount in the electrodeposition solution, leading to the results shown in Fig. S12B. If the Cz amount is too low, no modulation can be observed. Clearly the modulation is either absent (curve i) or unstable (curves ii and iii) below 5 %. Conversely, a reversible modulation can be observed for a Cz amount of 10 % (curve iv, identical to Fig. 6B), showing that in these conditions the polymer film behaves actually as an electrofluorochromic material.

The cycling ability of the poly(Rd-Cz) film with these optimal parameters (10 $\%_w$ Cz, 5 electropolymerization cycles) was tested for a potential modulation between 0 and 1.5 V (Fig. S13). While the modulation remains visible up to 25 cycles, the amplitude varies with a progressive fading. This means that optimization of the conditions is still to be done to improve the long-term stability, in view of possible applications.

In situ polymerization. Finally, the gradual emission quenching observed upon oxidation can be used to follow the electropolymerization process itself. Indeed, electropolymerization is performed under oxidative conditions to generate the cation radicals necessary for the coupling mechanism and thus the fluorescence intensity is expected to decrease as soon as the electropolymerization starts. This is precisely what is observed when electropolymerization occurs under potentiostatic conditions (Fig. 7A). When exciting at the maximal absorption wavelength of Rd (560 nm), the emission intensity recorded at 640 nm decreases as soon as the current starts to flow (Fig. 7B), which can be used to detect optically the

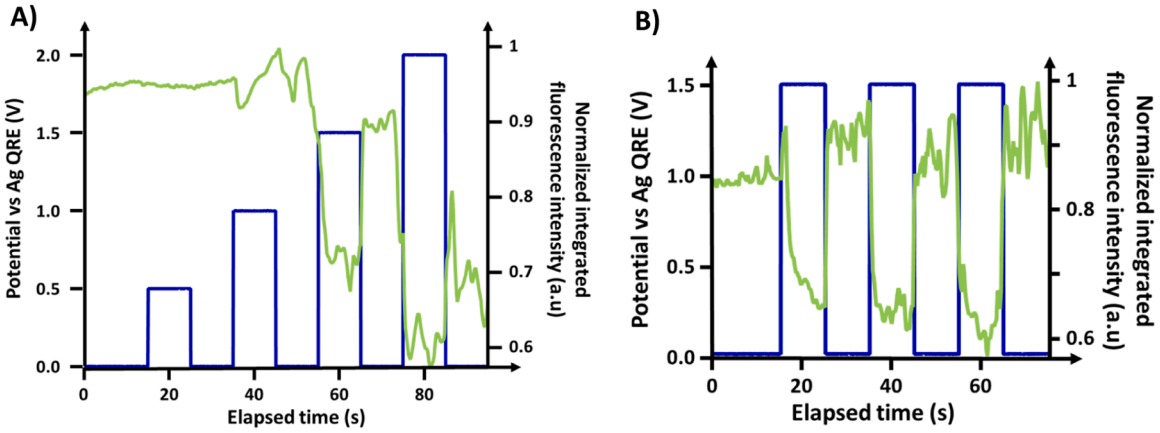

Fig. 6. Fluorescence intensity modulation of poly(RdCz) made with 10 % Cz and 5 cycles (160 nm thick) in DCM: A) at variable potential (from 0.5 to 2.0 V); B) at fixed potential (1.5 V). Excitation wavelength: 560 nm.

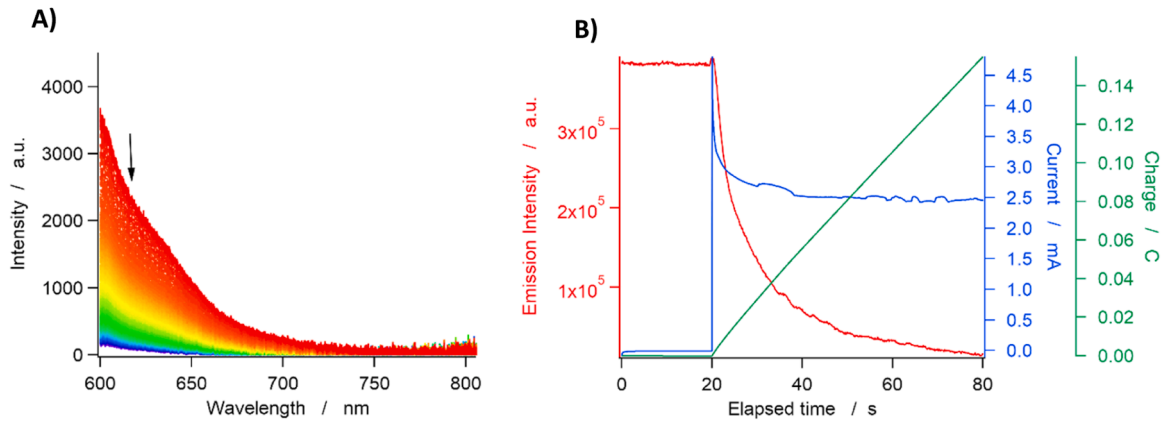

Fig. 7. A) Variation of fluorescence intensity upon electropolymerization at constant potential (1.5 V). Excitation wavelength: 560 nm. Emission wavelength: 640 nm. Composition of the reactional mixture RdCz 0.01 M + 10 % Cz in DCM. B) Emission intensity (red trace, from integrated spectrum), electrochemical current (blue trace) and electrochemical charge (green trace) for a potential step from 0 to 1.5 V.

electropolymerization start.

4. Conclusion

A rhodamine-carbazole dyad has been synthesized and electropolymerized to generate a conjugated polymer exhibiting both electrochromic and electrofluorochromic properties. We characterized the absorption properties of thin films at anodic potentials, demonstrating electrochromic properties due to a mixed contribution from the polycarbazole unit and the rhodamine moiety. Furthermore, we characterized for the first time the potential dependent emissive properties of these films, showing that reversible electrofluorochromism is possible but in a narrow range of potentials and film thickness. We provided guidelines to optimize the films, and experimental conditions in order to maximize the reversibility of the oxidative fluorescence quenching, with remaining work to be done to improve the long-term cyclability. In particular, we showed that the amount of carbazole in the electropolymerization medium and the film thickness are important parameters which greatly influence the final electrofluorochromic properties of the polymer. It is also shown that emission modulation involves at least partly the direct oxidation of the rhodamine unit in the conjugated backbone, an unexpected result compared to previously reported studies where rhodamine was always used in reduction. Finally, the luminescence quenching has been used to follow the electropolymerization itself under potentiostatic conditions in complement to the electrochemical current.

Besides highlighting the interest of this class of compounds for functional materials, this work demonstrates the importance of in situ microscopy techniques for analyzing the optical properties of smart materials.

CRediT authorship contribution statement

Jean-Frédéric Audibert: Formal analysis, Data curation. **Isabelle Bonnamour:** Supervision, Conceptualization. **Philippe Decorse:** Investigation. **Vitor Brasiliense:** Writing – review & editing, Supervision, Conceptualization. **Ulrich Darbost:** Supervision, Methodology, Conceptualization. **Florian Guier:** Investigation. **Roxanne Mollandin de Boissy:** Investigation. **Baptiste Maillot:** Investigation, Data curation. **Jennifer Calderon-Mora:** Investigation. **Fabien MIOMANDRE:** Writing – original draft, Supervision, Funding acquisition, Conceptualization.

Declaration of Competing Interest

The authors declare that they have no known competing financial interests or personal relationships that could have appeared to influence the work reported in this paper.

Acknowledgements

French National Research Agency (ANR APMJ ANR 19-CE09-0013) is acknowledged for funding the Master internship of J.C-M.

Appendix A. Supporting information

Supplementary data associated with this article can be found in the online version at doi:10.1016/j.synthmet.2024.117779.

Data availability

Data will be made available on request.

References

[1] P. Audebert, F. Miomandre, Electrofluorochromism: from molecular systems to set-up and display, Chem. Sci. 4 (2013) 575–584.
[2] Y. Watanabe, K. Nakamura, N. Kobayashi, Improvement in reflective-emissive dual-mode properties of electrochemical displays by electrode modification, PCCP 13 (2011) 19420–19426.
[3] J.W. Sun, Y.N. Chen, Z.Q. Liang, Electroluminochromic materials and devices, Adv. Funct. Mater. 26 (2016) 2783–2799.
[4] L. Lu, K. Wang, H. Wu, A. Qin, B.Z. Tang, Simultaneously achieving high capacity storage and multilevel anti-counterfeiting using electrochromic and electrofluorochromic dual-functional AIE polymers, Chem. Sci. 12 (2021) 7058–7065.
[5] G.A. Corrente, D.A. Gonzalez, E. Aktas, A.L. Capodilupo, G. Mazzone, F. Ruighi, G. Accorsi, D. Imbardelli, C. Rodriguez-Seco, E. Martinez-Ferrero, E. Palomares, A. Beneduci, Vis-NIR electrochromism and NIR-green electroluminochromism in dual functional benzothiadiazole-arylamine mixed-valence compounds, Adv. Opt. Mater. 11 (2023) 2301128.
[6] S.C. Yang, Y.T. Lin, J.W. Sun, C.J. Li, Y.J. Zhang, C. Zhang, Integrated electrochromic and electrofluorochromic properties from polyaniline-like polymers with triphenylacrylonitrile as side groups, Electrochim. Acta 421 (2022) 9.
[7] I. Seddiki, B.I. N'Diaye, W.G. Skene, Survey of recent advances in molecular fluorophores, unconjugated polymers, and emerging functional materials designed for electrofluorochromic use, Molecules 28 (2023) 42.
[8] F. Miomandre, How molecular electrochemistry may shine light by designing electrofluorochromic compounds, Curr. Opin. Electrochem. 24 (2020) 56–62.
[9] J. You, Y. Kim, E. Kim, Electrochemical fluorescence switching from anthracene polymer films, Mol. Cryst. Liq. Cryst. 520 (2010) 404–411.
[10] Y. Kim, J. Kim, J. You, E. Kim, Electrochemical modulation of color and fluorescence in one cell using conducting polymers, Mol. Cryst. Liq. Cryst. 538 (2011) 39–44.
[11] F. Montilla, R. Mallavia, In situ electrochemical fluorescence studies of PPV, J. Phys. Chem. B 110 (2006) 25791–25796.
[12] F. Montilla, L.M. Frutos, C.R. Mateo, R. Mallavia, Fluorescence emission anisotropy coupled to an electrochemical system: study of exciton dynamics in conjugated polymers, J. Phys. Chem. C 111 (2007) 18405–18410.

[13] L. Guerret-Legras, P. Audebert, J.F. Audibert, C. Niebel, T. Jarrosson, F. Serein-Spirau, J.P. Lere-Porte, New TBT based conducting polymers functionalized with redox-active tetrazines, J. Electroanal. Chem. 840 (2019) 60–66.
[14] C.-P. Kuo, Y.-S. Lin, M.-k Leung, Electrochemical fluorescence switching properties of conjugated polymers composed of triphenylamine, fluorene, and cyclic urea moieties, J. Polym. Sci. Part A 50 (2012) 5068–5078.
[15] S. Halder, N. Gupta, R.P. Behere, B.K. Kuila, C. Chakraborty, Vis-to-NIR electrochromism and bright-to-dark electrofluorochromism in a triazine and thiophene-based three-dimensional covalent polymer, Mol. Syst. Des. Eng. 7 (2022) 1658–1669.
[16] Y. Li, Y. Zhou, X. Jia, D. Chao, Synthesis and characterization of a dual electrochromic and electrofluorochromic crosslinked polymer, Eur. Polym. J. 106 (2018) 169–174.
[17] J.W. Sun, Z.Q. Liang, Swift electrofluorochromism of donor-acceptor conjugated polytriphenylamines, ACS Appl. Mater. Int. 8 (2016) 18301–18308.
[18] C.-P. Kuo, C.-L. Chang, C.-W. Hu, C.-N. Chuang, K.-C. Ho, M.-k Leung, Tunable electrofluorochromic device from electrochemically controlled complementary fluorescent conjugated polymer films, ACS Appl. Mater. Int. 6 (2014) 17402–17409.
[19] A.L. Capodilupo, F. Manni, G.A. Corrente, G. Accorsi, E. Fabiano, A. Cardone, R. Giannuzzi, A. Beneduci, G. Gigli, Arylamino-fluorene derivatives: optically induced electron transfer investigation, redox-controlled modulation of absorption and fluorescence, Dyes Pigments 177 (2020).
[20] R. Aoun, A. Yassin, M.El Jamal, A. Kanj, J. Rault-Berthelot, C. Poriel, Synthesis of a fluoresceine-derivatized fluorene and its electrogenerated copolymers with fluorene: new pH indicators, Synth. Met. 158 (2008) 790–795.
[21] J.S. Yu, T.Y. Zhou, The electrochemistry and thin-layer luminescence spectroelectrochemistry of rhodamine 6G at a 4,4 '-bipyridine-modified gold electrode, J. Electroanal. Chem. 504 (2001) 89–95.
[22] G.A. Corrente, A. Beneduci, Overview on the recent progress on electrofluorochromic materials and devices: a critical synopsis, Adv. Opt. Mater. 8 (2020) 2000887.
[23] X.J. Wang, L.X. Guo, L.H. Feng, A multi stimuli responsive material with rhodamine B and carbazole groups, New J. Chem. 43 (2019) 4181–4187.
[24] R. Ayranci, M. Ak, Synthesis of rhodamine and carbazole based conductive polymer for fluorescence and electrochromic applications, J. Electrochem. Soc. 164 (2017) H509–H514.
[25] R. Ayranci, D.O. Demirkol, S. Timur, M. Ak, Rhodamine-based conjugated polymers: potentiometric, colorimetric and voltammetric sensing of mercury ions in aqueous medium, Analyst 142 (2017) 3407.
[26] F. Miomandre, E. Lepicier, S. Munteanu, O. Galangau, J.F. Audibert, R. Meallet-Renault, P. Audebert, R.B. Pansu, Electrochemical monitoring of the fluorescence emission of tetrazine and bodipy dyes using total internal reflection fluorescence microscopy coupled to electrochemistry, ACS Appl. Mater. Interfaces. 3 (2011) 690–696.
[27] a) M. Cízková, L. Cattiaux, J.M. Mallet, E. Labbé, O. Buriez, Electrochemical switching fluorescence emission in rhodamine derivatives, Electrochim. Acta 260 (2018) 589–597;
b) T. Slanina, T. Oberschmid, Rhodamine 6G radical: a spectro (fluoro) electrochemical and transient spectroscopic study, ChemCatChem 10 (2018) 4182–4190.
[28] M. Wahl, Time-correlated single photon counting, Tech. Note, 2014.
[29] Jyoti, Evgenia Dmitrieva, Teresa Żołek, Dorota Maciejewska, Renata Rybakiewicz-Sekita, W.łodzimierz Kutner, Krzysztof R. Noworyta, An insight into the polymerization process of the selected carbazole derivatives – why does it not always lead to a polymer formation? Electrochim. Acta 429 (2022) 140948.
[30] F.O. Kirbay, R. Ayranci, M. Ak, D.O. Demirkol, S. Timur, Rhodamine functionalized conducting polymers for dual intention: electrochemical sensing and fluorescence imaging of cells, J. Mater. Chem. B 5 (2017) 7118.
[31] C. Chevrot, E. Ngbilo, K. Kham, S. Sadki, Optical and electronic properties of undoped and doped poly(N-alkylcarbazole) thin layers, Synth. Met. 81 (1996) 201–204.
[32] E. Contal, S. Lakard, F. Dumur, B. Lakard, Investigation of polycarbazoles thin films prepared by electrochemical oxidation of 3- and 9-substituted carbazoles, Prog. Org. Coat. 162 (2022) 106563.
[33] P.J. Peerce, A.J. Bard, Polymer films on electrodes: Part III. Digital simulation model for cyclic voltammetry of electroactive polymer film and electrochemistry of poly(vinylferrocene) on platinum, J. Electroanal. Chem. 114 (1980) 89–115.
[34] A.J. Bard, L.R. Faulkner, Electrochemical Methods Fundamentals and Applications, John Wiley & Sons, Inc, 2001.
[35] S. Cosnier, A. Karyakin, Electropolymerization. Concepts, Materials and Applications, Wiley-VCH2010.
[36] A.S. Sarac, M. Serantoni, S.A.M. Tofail, V.J. Cunnane, Morphological and spectroscopic analyses of poly N-vinylcarbazole-co-vinylbenzenesulfonic acid copolymer electrografted on carbon fiber: the effect of current density, Appl. Surf. Sci. 229 (2004) 13–18.